Available online at www.sciencedirect.com
ScienceDirect
Journal of Organometallic Chemistry 692 (2007) 2282–2290
Journal of Organometallic Chemistry
www.elsevier.com/locate/jorganchem

Mechanism of olefin hydrosilylation catalyzed by $[RuCl(NCCH_3)_5]^+$: A DFT study

Tell Tuttle [a,*], Dongqi Wang [a], Walter Thiel [a,*], Jutta Köhler [b], Marco Hofmann [b], Johann Weis [b]

[a] Max-Planck-Institut für Kohlenforschung, D-45470 Mülheim an der Ruhr, Germany
[b] Consortium für Elektrochemische Industrie GmbH, Zielstattstrasse 20, D-81379 München, Germany

Received 14 November 2006; accepted 30 January 2007
Available online 11 February 2007

Abstract

The hydrosilylation reaction between methyldimethoxysilane and methylvinyldimethoxysilane, catalyzed by the cationic species chloropenta(acetonitrile)ruthenium(II)$^+$ (**C1**), was investigated with density functional theory (DFT). The Chalk–Harrod, Glaser–Tilley and σ-bond metathesis mechanisms were considered as mechanistic possibilities for the reaction and enthalpy profiles of each pathway were computed for the active form of **C1**. In contrast to the commonly accepted Chalk–Harrod mechanism of hydrosilylation, the computational results indicate that a σ-bond metathesis mechanism, involving the formation of a hydride analogue of **C1**, is most favored. The B3LYP calculated activation enthalpy for this pathway ($\Delta H_{act} = 13.1$ kcal/mol) is consistent with the experimental observation that **C1** is a reasonable catalyst for this reaction under the applied experimental conditions.

Keywords: Density functional theory; B3LYP; Ruthenium; Hydrosilylation; Chalk–Harrod mechanism; Glaser–Tilley mechanism; σ-Bond metathesis

1. Introduction

Hydrosilylation, the addition of hydrosilanes across unsaturated bonds [1–4], is an important reaction in the process of creating organosilicon building blocks. These building blocks are subsequently used in the construction of commercially available silicon based products, such as: silicone rubber, liquid injection molding compounds, paper release coatings, pressure sensitive adhesives, binders and coupling agents [2,5–7].

Hydrosilylation reactions are normally performed under mild conditions in the presence of a catalyst [1–4]. The most common catalysts for these reactions have traditionally been platinum based compounds owing to their high activity and the ability to control their reactivity by altering the experimental conditions [1–4,8]. One avenue for controlling the activity of platinum based compounds is through the manipulation of the active species generated in the induction phase [8]. This type of selectivity was successfully applied for a particular class of platinum based catalysts, bis(alkynyl)(1,5-cyclooctadiene)platinum complexes (COD)Pt(CCR)$_2$ [9].

Other transition metal compounds can catalyze the hydrosilylation reaction as well, e.g. those based on ruthenium [10–19]. However, such catalysts generally suffer from a loss of activity and/or selectivity relative to platinum catalysts, and they may induce side reactions of the substrates including olefin isomerization, dehydrogenative silylation and hydrogenation. Nonetheless, some very selective ruthenium catalysts have been found for the regioselective hydrosilylation of alkynes, especially the cationic ruthenium species $[Cp^*Ru(NCMe)_3]PF_6$ which has been extensively used by Trost and Ball [13,14]. Another ionic

* Corresponding authors. Tel.: +49 208 306 2163; fax: +49 208 306 2996 (T. Tuttle).
E-mail addresses: tell@mpi-muelheim.mpg.de (T. Tuttle), thiel@mpi-muelheim.mpg.de (W. Thiel).

0022-328X/$ - see front matter © 2007 Elsevier B.V. All rights reserved.
doi:10.1016/j.jorganchem.2007.01.060

ruthenium species, $[RuCl(NCCH_3)_5][RuCl_4(NCCH_3)_2]$ has been shown to be a very effective catalyst in the hydrosilylation of CO_2 with tri- and diorganosilanes [20,21]. These studies prompted us to investigate the activity of the latter catalyst in the hydrosilylation of C=C-functional substrates. A preliminary test reaction of diethoxymethylsilane with diethoxymethylvinylsilane indicated that the activity of the catalyst was indeed reasonable (see Section 2).

To optimize ionic catalysts such as $[RuCl(NCCH_3)_5][RuCl_4(NCCH_3)_2]$ it is essential to understand the catalytic mechanism. Thus, we present in this report the results of a computational investigation of the mechanism by which the Ru(II) cation $[RuCl(NCCH_3)_5]^+$ (**C1**) catalyzes the reaction between dimethoxymethylsilane (**R1**) and dimethoxymethylvinylsilane (**R2**) to form 1,2-bis(dimethoxymethylsilyl)ethane (**P1**), Scheme 1, as the first step towards the fine-tuning of the catalyst for optimal activity. We assume in our model calculations that the Ru(II) cation is the active species, rather than the Ru(III) anion $[RuCl_4(NCCH_3)_2]^-$, since there are no Ru(III) complexes among all known Ru hydrosilylation catalysts (excluding $RuCl_3$, which is not the active species itself).

The Chalk–Harrod [22] (CH) and modified Chalk–Harrod [16,23–27] (mCH) catalytic cycles are the most common mechanisms in the literature for explaining the catalysis of the hydrosilylation reaction with late transition metal based compounds [8,13,14,17,28–33]. Both the CH and mCH mechanisms involve an initial oxidative addition of an SiH-functional silane to the transition metal, Ru (step I, Scheme 2). In the CH mechanism, this is followed by subsequent insertion of a C=C functional substrate into the Ru–H bond (step IIa), whereas in the mCH mechanism the C=C bond is inserted into the Ru–Si bond (step IIb). The final step (step III) for both mechanisms is the reductive elimination of the hydrosilylation product.

An alternative to the Chalk–Harrod scheme is the σ-bond metathesis (SBM) mechanism [34,35], which is well established for early transition metal catalysts [36–40]. More recently, it has also been shown to be active in a number of late transition metal catalysts as well [19,41–51]. Finally, in 2003, Glaser and Tilley proposed another mechanism for a cationic silylene Ru(II) catalyst in the hydrosilylation of alkenes [11], and subsequent computational studies supported this proposal [10]. The Glaser–Tilley (GT) mechanism (Scheme 3) involves the insertion of the alkene directly into an Si–H bond remote from the metal center (i.e. no direct interaction between the alkene and Ru). Given the cationic nature of our catalyst, this mechanism was also tested.

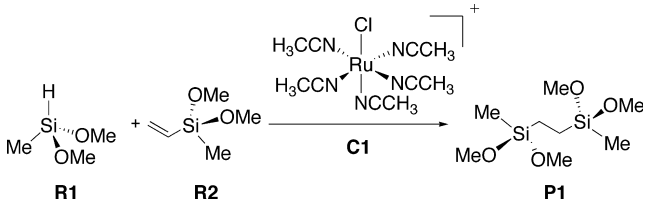

Scheme 1. Chemical structure and notation of the reactants, products and catalyst.

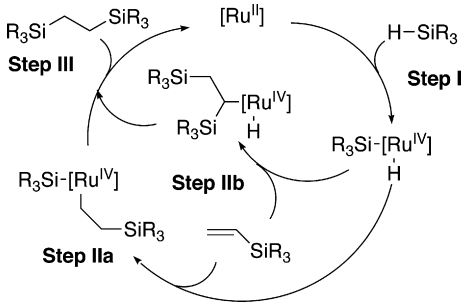

Scheme 2. Chalk–Harrod and modified Chalk–Harrod catalytic cycles.

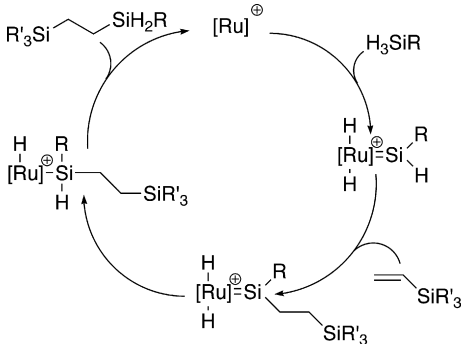

Scheme 3. Glaser–Tilley catalytic cycle.

2. Experimental

2.1. General considerations

The silanes diethoxymethylvinylsilane and diethoxymethylsilane were purchased from GELEST and used as received. The ruthenium catalyst $[RuCl(NCCH_3)_5][RuCl_4(NCCH_3)_2]$ was prepared by the method of Pitter et al. [20]. ^1H and ^{29}Si NMR spectra were recorded at room temperature on a Bruker Avance 300 spectrometer in $CDCl_3$. All chemical shifts are in ppm referenced to the residual proton solvent resonance at δ 7.24 ppm (^1H), or to the external standard TMS (^{29}Si). Routine GC analysis was performed with an AGILENT 6890 N gas chromatograph equipped with an RtX-200 column (Restek GmbH). Calibration was performed with pure samples of the silanes diethoxymethylvinylsilane, diethoxymethylsilane, and triethoxymethylsilane (purchased from GELEST) as well as bis(diethoxymethylsilyl)ethane, which was independently prepared by the literature method [52]. GC–MS spectra were measured on an AGILENT 6890/MSD 5973 GC/mass spectrometer at 70 eV.

2.2. Catalytic run

A 25 mL two-necked round-bottomed flask equipped with a reflux condenser, argon inlet and a magnetic stir-

ring bar was charged under argon with 17.1 mg (25.6 μmol) of $[RuCl(NCCH_3)_5][RuCl_4(NCCH_3)_2]$. A 1.75 g (10.9 mmol) amount of $Me(Vi)Si(OEt)_2$ and 1.46 g (10.9 mmol) of $Me(H)Si(OEt)_2$ were added by syringe and the mixture was stirred and heated at 100 °C. The progress of the reaction was monitored by GC. After 2 h the starting SiH-functional silane was completely consumed. After cooling to room temperature, the reaction mixture was analyzed by GC and GC/MS. The crude mixture was purified by distillation leaving pure $(EtO)_2MeSi–CH_2CH_2–SiMe(OEt)_2$ in a yield of 1.77 g (55%). The ^1H NMR data of $(EtO)_2MeSi–CH_2CH_2–SiMe(OEt)_2$ compare well with the literature values [53].

2.3. $(EtO)_2MeSi–CH_2CH_2–SiMe(OEt)_2$

^1H NMR (300.1 MHz, $CDCl_3$) δ 3.72 (q, 8H, $J = 7.0$ Hz, H_2CO), 1.17 (t, 12H, $J = 7.0$ Hz, H_3CCH_2), 0.54 (s, 4H, CH_2CH_2), 0.07 (s, 6H, H_3CSi). ^{29}Si NMR (59.6 MHz, $CDCl_3$) δ −4.42 (s). GC/MS: m/z (relative abundance): 279 (4%, $M-CH_3$).

2.4. Reaction products

The hydrosilylation of diethoxymethylvinylsilane with diethoxymethylsilane was performed at 100 °C in the presence of $[RuCl(NCCH_3)_5][RuCl_4(NCCH_3)_2]$ (0.0024 equiv.) without solvent monitoring the progress of the reaction via GC. After 2 h, no hydrosilane was detectable by GC. However, the formation of the hydrosilylation product $(EtO)_2MeSi–CH_2CH_2–SiMe(OEt)_2$ (60% yield by GC) is accompanied by several by-products, especially $MeSi(OEt)_3$ (12%), presumably as a result of a H/OEt exchange reaction of diethoxymethylsilane. This would also explain that diethoxymethylvinylsilane is not fully consumed (7% left in the reaction mixture). The product distribution also contains 21% of unidentified compounds. However, it is noteworthy that the product of a dehydrogenative silylation, i.e. $(EtO)_2MeSi–CH{=}CH–SiMe(OEt)_2$ [54] is not formed, which implies that a β-hydrogen elimination reaction as side reaction path consecutively to step IIb in Scheme 2 (according to the modified Chalk–Harrod mechanism) does not occur. This may also imply that the mCH mechanism is not valid for this catalyst (see below).

3. Computational methods

Density functional theory (DFT) [55,56] was employed for the calculation of all reactants, transition states (TSs), intermediates and products. In all calculations, the ruthenium atom was described by a small-core, quasi-relativistic, effective core potential with the associated (7s6p5d)/[5s3p3d] valence basis set [57], while the 6-31G(d,p) basis set [58–60] was used for all other atoms. Initial geometry optimizations of the minima along the reaction path were performed with the gradient-corrected BP86 functional [61–63], in order to take advantage of the resolution-of-the-identity (RI)-DFT approach [64], as implemented in TURBOMOLE [65–68]. All structures were subsequently refined in GAUSSIAN-03 [69], by carrying out geometry optimizations with the B3LYP hybrid functional [61,63,70–73], which has been shown to produce reliable thermochemical data for ruthenium-based compounds [74–76].

GAUSSIAN-03 was employed in the refinement process as the search for TSs often made use of the synchronous transit-guided quasi-Newton method [77,78], available in this package. Frequency calculations were performed on all optimized structures, using the B3LYP functional, to characterize the stationary points as minima or TSs, as well as for the calculation of zero-point energies (ZPE), enthalpies (H), entropies (S), and Gibbs free enthalpies (G) at 298 K.

4. Results and discussion

The addition of **R1** to **R2** in an uncatalyzed hydrosilylation reaction occurs in a concerted mechanism, with the H-abstraction from **R1** and the Si–C bond formation occurring concomitantly. In our previous study [19], this reaction was found to have a prohibitively high barrier ($\Delta H_{act} = 53.6$ kcal/mol) and a catalyst is therefore needed to lower the activation enthalpy for the hydrosilylation to occur under normal operating conditions.

4.1. The catalyst

The cation **C1** is produced as an ion pair [20,21] – *trans*-$[Ru^{II}Cl(MeCN)_5][Ru^{III}Cl_4(MeCN)_2]$ – with a Ru(II) cation and a Ru(III) anion, from the reaction of $RuCl_3$ with dimethylphenylsilane in acetonitrile. As mentioned before, we only consider the Ru(II) cation **C1** as catalyst for the hydrosilylation reaction.

The optimized structure of **C1** (Fig. 1) is in good agreement with the available X-ray structure. The average Ru–N bond length, *cis* to the Ru–Cl bond, is 2.03 Å, in excellent agreement with the reported X-ray structure value (2.03 Å)

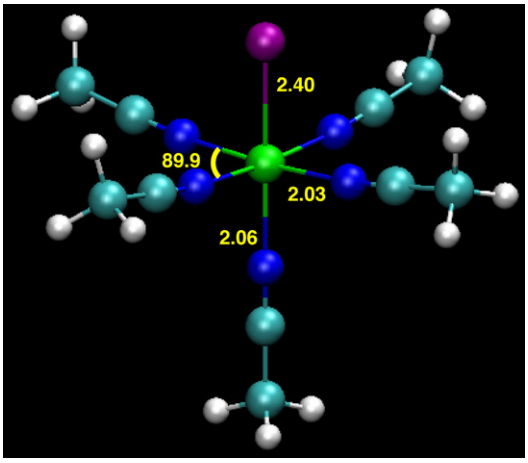

Fig. 1. Optimized structure of **C1**. Bond length in Å and angles in °.

[20]. The agreement between the computed and X-ray structure is equally good for the Ru–Cl bond (2.40 Å). The computed structure has a slightly elongated Ru–N bond in *trans* position to the Cl ligand (2.06 Å), consistent with the strong σ-donor capabilities of the chloride ligand. In the X-ray structure (Ru–N = 2.02 Å) such an elongation was not observed. Nonetheless, the overall agreement between the computed and X-ray structure is excellent and indicates that the current level of theory is capable of adequately describing the cationic Ru(II) catalyst.

4.2. The induction period

Generating the active form of **C1** requires the dissociation of at least one of the six ligands in the octahedral complex. In the classic version of the CH or mCH mechanisms, two free coordination sites are required to bind the reaction partners. The dissociation enthalphy (ΔH_d (298 K)) for removing two acetonitrile ligands is 70.5 kcal/mol, hence this process is prohibitive enthalpically (Scheme 4).

An alternative induction mechanism begins with the replacement of one of the acetonitrile ligands by R1, which yields the hexa-coordinated complex **C4** (Fig. 2). The direct substitution via the transition state **TS(C1–C4)** requires an activation of 23.5 kcal/mol and is thus enthalpically more favorable than the corresponding dissociation/association mechanism, which has an enthalpic cost of 31.2 kcal/mol for the initial dissociation **C1** → **C2** while the subsequent addition **C2** + **R1** → **C4** is barrierless and exothermic. The complex **C4** is destabilized by 13.4 kcal/mol relative to **C1**. It can be transformed into a more active form (**C5**) by a slightly exothermic σ-bond metathesis reaction ($\Delta H = -2.3$ kcal/mol), in which the Si–H bond of **R1** is replaced by the Si–Cl bond, and the Ru–Cl bond by the Ru–H bond (via **TS(C4–C5)**, $\Delta H_{act} = 12.2$ kcal/mol). The hexa-coordinated complex **C5** can lose the chlorosilane ligand rather easily ($\Delta H = 8.9$ kcal/mol) to form the penta-coordinated complex **C7** (see below). Both **C5** and **C7** are thus enthalpically accessible and can serve as starting points for the catalytic cycle.

In a recent study [19] of the same hydrosilylation reaction with the $RuCl_2(CO)_2(PPh_3)_2$ catalyst (**A1**), the initial dissociation of a triphenylphosphine ligand was found to be much more facile, with an enthalpic cost of only 15.4 kcal/mol, i.e. about half of that required for removing an acetonitrile ligand from the current catalyst **C1**. This difference is due to the electron-deficient Ru(II) environment created by the acetonitrile ligands in **C1**. In the previous study [19], the active form of the catalyst (**A16**) was generated by a subsequent direct σ-bond metathesis reaction between the dissociation product $RuCl_2(CO)_2(PPh_3)$ (**A7**) and **R1** which required only very little activation ($\Delta H_{act} = 1.9$ kcal/mol) followed by a rearrangement of the resulting penta-coordinated complex $RuHCl(CO)_2(PPh_3)$ (**A8**). The induction mechanisms for the previously and presently studied catalysts thus show some similarities: the active species **C7** and **A16** are analogous penta-coordinated complexes that contain a Ru–H bond which is introduced by a chloride/hydride exchange through a σ-bond metathesis reaction with **R1**. However, there are also differences: in the present case, additional hexa-coordinated complexes (**C4** and **C5**) are encountered on the induction pathway, and in the initial induction step (**C1** → **C4**), a direct substitution is enthalpically favored because of the higher barrier to ligand dissociation. The induction is enthalpically less facile in the present case, since the largest single-step activation enthalpies are 15.4 and 23.5 kcal/mol for **A1** and **C1**, respectively, while the highest points on the corresponding enthalpy profiles are 17.3 and 25.6 kcal/mol, respectively. Under the normally applied experimental conditions, such barriers are surmountable in the induction phase.

In the following, we address three possible catalytic mechanisms for our current catalyst: the CH and GT mechanisms starting from **C5**, and an SBM mechanism starting from **C7**. The role of entropic effects will be discussed thereafter.

4.3. Catalytic mechanisms

The CH mechanism involves the insertion of an alkene into the metal-hydride bond followed by the product forming step where the metal–silyl bond is broken (Scheme 2). In **C5** the alkene (**R2**) is able to insert into the Ru–H bond (Fig. 3) to form **C6**. However, a Ru–Si bond does not exist in **C5**, which excludes the mCH mechanism (Scheme 2) for this active species. The optimized mCH intermediate, constructed from the four-coordinate Ru(II) complex, is 23.8 kcal/mol less stable than the analogous CH intermediate. Thus, the relative stability of the two intermediates also disfavors the possibility of an mCH mechanism for this catalyst.

The insertion of **R2** into **C5** to form the CH intermediate is an exothermic reaction (ΔH(**C6**) = −6.8 kcal/mol) but requires the surmounting of an extremely large barrier (ΔH_{act}(**TS(C5–C6)**) = 56.7 kcal/mol). The high activation enthalpy for the olefin insertion process arises from the steric crowding around the metal center. The approaching olefin is not able to form a pre-complex with the metal before abstracting the hydride due to the saturation of the coordination sites in **C5** (Fig. 4). Consequently, the hydride abstraction precedes the formation of the Ru–C bond in **C6**, which is a highly unfavorable process given the electron deficient acetonitrile environment. This is in contrast to our findings on the $RuCl_2(CO)_2(PPh_3)_2$ catalyst where the metal center had been oxidized to a Ru(IV) state

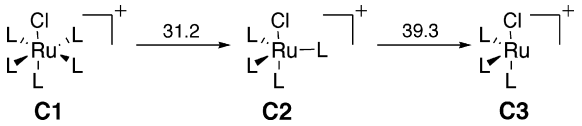

Scheme 4. Dissociation of acetonitrile ligands (L = NCMe), dissociation enthalpy ΔH_d (298 K) given in kcal/mol.

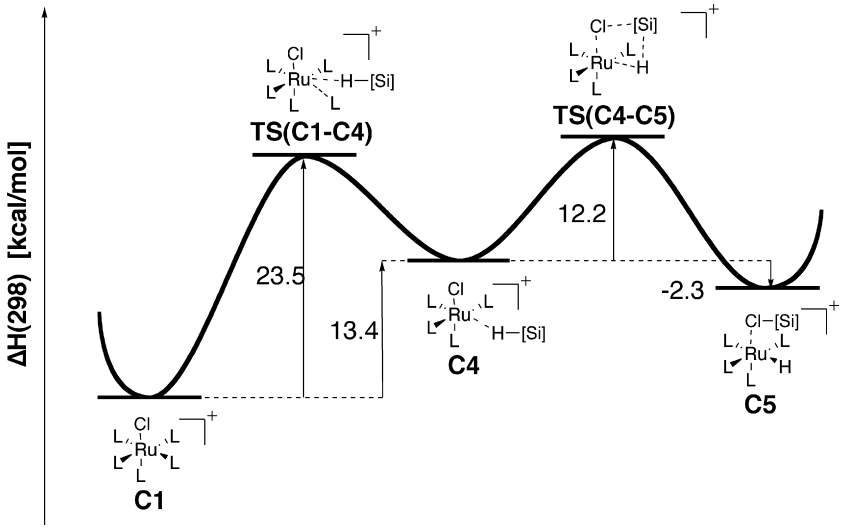

Fig. 2. Induction mechanism for **C1**: Replacement of an acetonitrile ligand by **R1**. L: NCMe, [Si]: $Si(OMe)_2Me$.

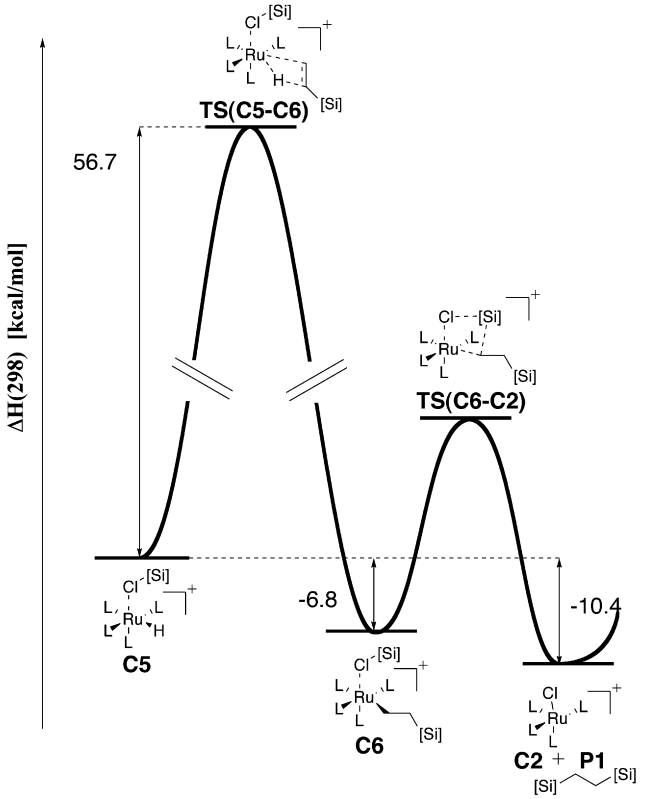

Fig. 3. Enthalpy profile for the CH mechanism. L: NCMe, [Si]: $Si(OMe)_2Me$.

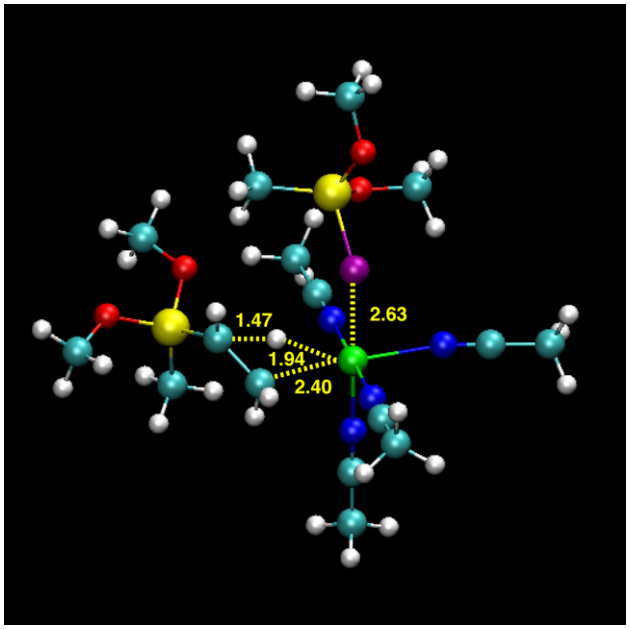

Fig. 4. TS structure for the olefin insertion in the CH mechanism. Bond lengths in Å.

upon addition of the silane in the CH mechanism [19]. The abstraction of the hydride to form the CH intermediate therefore occurred with only a small barrier (6.7 kcal/mol), although, the final reductive elimination step excluded the CH mechanism for this catalyst as well [19]. In the current catalyst it is the barrier to forming the CH intermediate that excludes this mechanism as a viable pathway for the hydrosilylation reaction. Therefore, we did not invest time into obtaining the TS of the product forming step, although the reaction is again exothermic (ΔH(**C2**) = −3.6 kcal/mol).

The GT mechanism also requires a formal metal–silyl bond in its original form [11]. Nonetheless, in **C5** the hydride and silyl groups are well positioned to allow them to interact directly with **R2**, even though there is no binding between **R2** and the metal center in the GT-type TS (Fig. 5). The simultaneous abstraction of both the silyl and hydride ligands leads directly to **P1** and the active form of the catalyst, **C2**. The addition of **R1** to **C2** occurs in a barrierless reaction (ΔH(**C4**) = −17.8 kcal/mol) to generate **C4** (see Fig. 2). However, the activation enthalpy for this

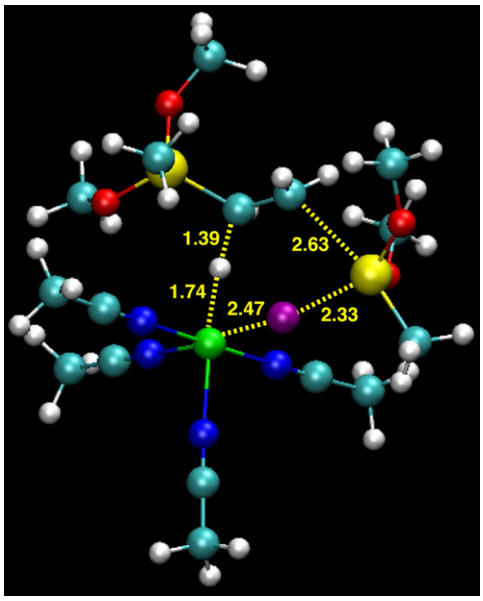

Fig. 5. TS structure for the GT-type mechanism. Bond lengths in Å.

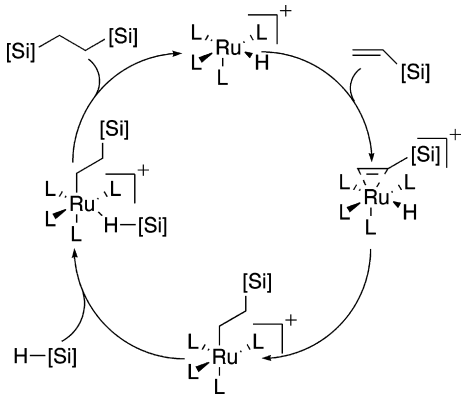

Scheme 5. SBM catalytic mechanism. L: NCMe, [Si]: $Si(OMe)_2Me$.

reaction is 47.4 kcal/mol, which is clearly too high to explain the observed catalytic activity of this catalyst.

Generally, silyl ligands have strong σ-donor tendencies; in the GT mechanism (Scheme 3) the electron donation to the metal centre is enhanced by forming a double bond to the metal center. This electron donation weakens the Si–H bond, which allows the alkyl group to abstract the H-atom from Si and form a Si–C bond. That is, by forming a double bond to the metal center the Si-atom is activated and consequently the barrier is lowered for the hydrosilylation reaction. In **C3** the Si-atom has not been activated by Ru, rather the interaction between the Ru- and Si-atoms is very weak and the chlorosilane ligand is energetically stable. The barrier to the hydrosilylation reaction in this mechanism is therefore only slightly lower than in the uncatalyzed reaction ($\Delta H_{act} = 53.6$ kcal/mol) [19].

The CH and GT-type pathways discussed above provide helpful insights to the requirements that the actual mechanism must fulfill. To wit, an additional free coordination site is required to allow enough space around the metal center for the reactants to interact with Ru; and, at least **R1** or **R2** must directly bind to the metal center in order to lower the activation barrier. We have incorporated these features into a catalytic mechanism that is based on a series of SBM reactions (Scheme 5).

The active species in this mechanism is **C7** (Fig. 6) which is generated from **C5** by the liberation of chlorosilane in an endothermic process ($\Delta H(\mathbf{C7}) = 8.9$ kcal/mol). The olefin is able to bind to **C7** in a barrierless, exothermic reaction to form **C8** ($\Delta H(\mathbf{C8}) = -29.5$ kcal/mol). The intramolecular H-transfer reaction to form **C9** occurs with a low barrier ($\Delta H_{act}(\mathbf{TS(C8–C9)}) = 6.9$ kcal/mol), however, the intermediate alkyl-ruthenium complex is produced in an endothermic reaction ($\Delta H(\mathbf{C9}) = 5.3$ kcal/mol). The free coordination site in **C9** is amenable to the attack of **R1**, which stabilizes the complex by 2.4 kcal/mol via a dative bond involving its hydrogen atom (**C10**, Fig. 6) in an unhindered process. The last step in the catalytic cycle is the rate-determining step. The creation of the product occurs through a final SBM reaction where the H–Si bond in **C10** is replaced by the C–Si bond in **P1** and the Ru–C bond is replaced by a Ru–H bond as the active species, **C7**, is reformed.

This catalytic mechanism is analogous to that in the previously studied catalyst [19]. However, contrary to the induction period, the present catalyst is predicted to be more efficient in the catalytic cycle, particularly with regard to the rate-determining product formation step. The overall barrier in the catalytic cycle for the current catalyst ($\Delta H_{act} = 16.0$ kcal/mol, relative to **C8**), is significantly lower than that obtained for the $RuCl_2(CO)_2(PPh_3)_2$ catalyst ($\Delta H_{act} = 21.8$ kcal/mol) [19], which reflects the activity ordering obtained experimentally for the two systems. The differences in the barrier heights during induction thus do not play a significant role in determining the catalytic ability of the two compounds – it is the product formation step in the catalytic cycle that is decisive.

4.4. Entropic effects

Equilibria and reaction rates depend on the Gibbs free enthalpies, which differ from the reported relative enthalpies (ΔH) through the inclusion of the entropic contributions ($\Delta G = \Delta H - T\Delta S$). These contributions have been calculated by applying the harmonic oscillator/rigid rotor approximation (see Supplementary material); however, the results should be viewed with some caution, for two reasons. First, the computed entropic contributions refer to the gas phase and thus neglect solvation and desolvation effects in solution, which may be substantial. Second, the harmonic oscillator/rigid rotor approximation is known to be problematic in the case of weakly bound complexes (such as **C4** and **C10**) due to the large number of low-energy vibrational modes, which in turn have large contributions to the entropy. Therefore, the following discussion

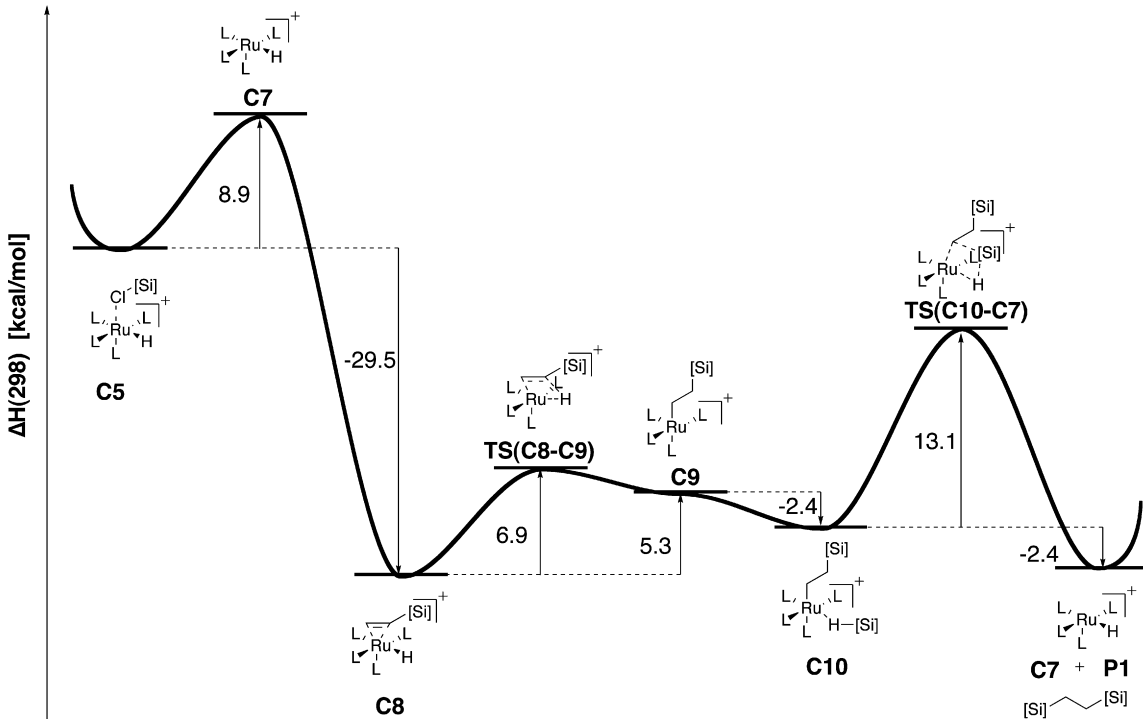

Fig. 6. Enthalpy profile for the SBM mechanism. L: NCMe, [Si]: $Si(OMe)_2Me$.

focuses on how the computed enthalpy profile (Fig. 7) is qualitatively affected by the entropic contributions. The main such effect is that association reactions suffer from an entropic penalty because of the loss of translational and rotational degrees of freedom (typically around 10 kcal/mol at 298 K in the gas phase), while dissociation reactions are entropically favored in an analogous manner. In solution, these entropic effects will be less pronounced than in the gas phase due to solvation and desolvation, but they will be present to some extent.

In the induction phase (Fig. 7, black part) the direct substitution of acetonitrile (**C1** → **C4**) becomes less facile on the ΔG scale because of the entropic contributions associated with the loss of rotational and translational freedom when coordinating **R1** (i.e. **TS(C1–C4)** is a seven coordinate complex). However, on the ΔG scale the dissociation

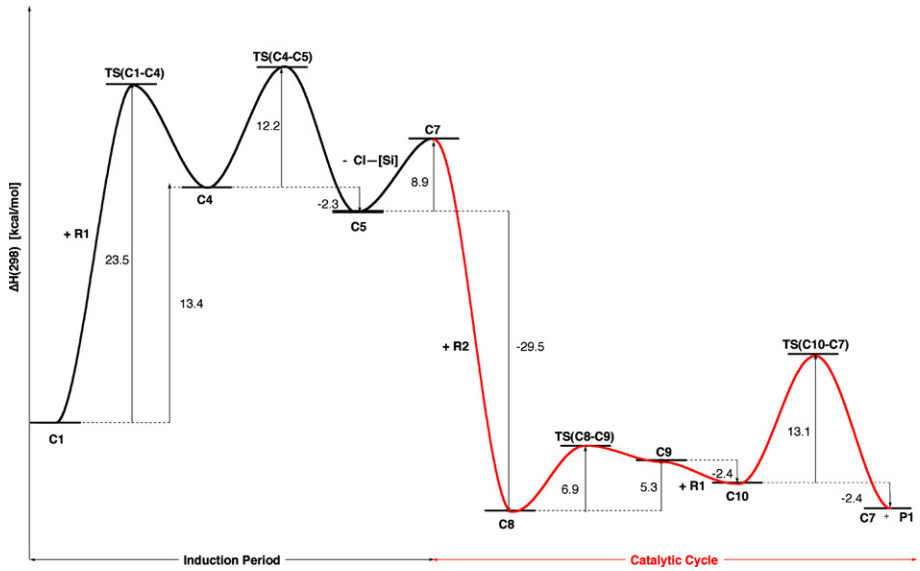

Fig. 7. Relative enthalpy profile of the predicted mechanism for the hydrosilylation of **R2** by **R1** with the **C1** catalyst. Induction period in black, catalytic cycle in red. The numerical values given are barriers in the case of the TSs and reaction enthalpies relative to the preceding minimum otherwise (kcal/mol). (For interpretation of the references to colour in this figure legend, the reader is referred to the web version of this article.)

of one of the acetonitrile ligands to form **C2** becomes more favorable (ΔG(**C2**) = 21.2 kcal/mol). The subsequent association of **R1** remains as an unhindered process, although it is not as stabilizing on the ΔG scale due to the destabilizing entropic contribution (**C2** → **C4**: $\Delta H = -17.8$ kcal/mol, $\Delta G = -5.5$ kcal/mol). Thus, the inclusion of entropic effects should lead to a change in the preferred mechanism for the formation of **C4** from a direct mechanism (**C1** → **C4**), which is favored enthalpically, to a dissociation/association mechanism (**C1** → **C2** → **C4**), which is more facile when free enthalpies are considered.

The SBM reaction in the induction step (**C4** → **C5**) is not significantly affected by the inclusion of entropic effects ($\Delta H_{act} = 12.2$ kcal/mol, $\Delta G_{act} = 14.8$ kcal/mol) due to the intramolecular nature of the reaction. The dissociation of chlorosilane in the formation of **C7** is favored from an entropic perspective (**C5** → **C7**: $\Delta H = 8.9$ kcal/mol, $\Delta G = -3.0$ kcal/mol). On the ΔG scale, formation of **C4** thus remains as the rate-determining step of the induction phase, and the five-coordinate intermediate (**C7**), formed in the latter part of the reaction, is entropically favored.

Considering the SBM catalytic cycle (Fig. 7, red part[1]) we first note that the overall reaction (**C7** + **R1** + **R2** → **C7** + **P1**) combines two reactant molecules into one product molecule so that the entropic contributions must be positive, which is indeed found ($\Delta H = -29.0$ kcal/mol, $T\Delta S = 12.9$ kcal/mol, $\Delta G = -16.1$ kcal/mol). Similarly, the intermediates in the SBM catalytic cycle (**C8** + **R1**, **C9** + **R1**, **C10**) all have fewer molecules than the entry point (**C7** + **R1** + **R2**). Therefore, in the ΔG profile of the catalytic cycle, all intermediates and the product are shifted upwards compared with the ΔH profile, but the other features remain qualitatively unchanged. In particular, the barrier to form the alkyl intermediate (**C9**) remains similar on the ΔH and ΔG scales, and product formation remains as the rate-determining step. The qualitative conclusions drawn from the ΔH profile (Fig. 7) thus remain valid also after considering entropic effects in the catalytic cycle.

5. Conclusions

The comparison of the different reaction mechanisms involving **C1** shows that the SBM mechanism provides the most favorable route to the hydrosilylation of **R2** by **R1**. The induction period of the catalyst involves the replacement of an acetonitrile ligand (either by a substitution reaction or a dissociation/association process) by **R1**, followed by a SBM reaction that causes the exchange of the H-atom of **R1** for the Cl-atom and introduces a hydride ligand on the metal center (**C5**). In the induction phase, the direct substitution of an acetonitrile ligand by **R1** has an activation enthalpy of 23.5 kcal/mol. The initial dissociation of an acetonitrile followed by the association of **R1** to form **C4** is more favorable from a free enthalpy perspective ($\Delta H_{act} = 31.2$ kcal/mol; $\Delta G_{act} = 21.1$ kcal/mol). Thus, either of these induction mechanisms are clearly favored over the spontaneous dissociation of two acetonitrile ligands due to the electron deficient environment of Ru(II).

The subsequent dissociation of the chlorosilane to form **C7** represents the starting point of the SBM catalytic mechanism. A stabilizing η^2-coordination of **R2** (−29.5 kcal/mol) in a barrierless reaction initiates the catalytic cycle, where the initial transformations (**C7** → **C8** → **C9** → **C10**) are facile. The final SBM step that generates the product (**C10** → **C7**) is rate-determining and the corresponding barrier of $\Delta H_{act} = 13.1$ kcal/mol ($\Delta G_{act} = 22.5$ kcal/mol) is consistent with the experimentally observed activity.

[1] For interpretation of the references to colour in Fig. 7, the reader is referred to the web version of this article.

Acknowledgement

We thank Dr. Hans-Jürgen Eberle for helpful discussions.

Appendix A. Supplementary material

Energies, thermochemical data and Cartesian coordinates of all optimized structures and the complete Ref. [69] are provided as supplementary material. Supplementary data associated with this article can be found, in the online version, at doi:10.1016/j.jorganchem.2007.01.060.

References

[1] D. Armitrage, in: G. Wilkinson, F.G.A. Stone, W.E. Abel (Eds.), Comprehensive Organometallic Chemistry, Pergamon Press, Oxford, 1982, p. 117.
[2] B. Marciniec, J. Gulinski, W. Urbaniak, Z.W. Kornetka, Comprehensive Handbook on Hydrosilylation;, Pergamon Press, Oxford, 1992.
[3] I. Ojima, in: S. Patai, Z. Rappoport (Eds.), The Chemistry of Organic Silicon Compounds, Wiley, New York, 1989, p. 1479.
[4] J.L. Speier, in: F.G.A. Stone, W.E. Abel (Eds.), Advances in Organometallic Chemistry, Academic Press, New York, 1979, p. 407.
[5] L.N. Lewis, J. Stein, Y. Gao, R.E. Colborn, G. Hutchins, Platinum Met. Rev. 41 (1997) 66.
[6] W. Noll, Chemistry and Technology of Silicones, Academic Press, New York, 1968.
[7] F.O. Stark, J.R. Falender, A.P. Wright, in: G. Wilkinson, F.G.A. Stone, W.E. Abel (Eds.), Comprehensive Organometallic Chemistry, Pergamon Press, Oxford, 1982, p. 306.
[8] M.N. Jagadeesh, W. Thiel, J. Köhler, A. Fehn, Organometallics 21 (2002) 2076.
[9] A. Fehn, F. Achenbach, E.P. Appl, Curable Silicone Rubber Compositions Containing Organoplatinum Catalysts, Wacker-Chemie GmbH, Germany, 2000, EP 994159.
[10] C. Beddie, M.B. Hall, J. Am. Chem. Soc. 126 (2004) 13564.
[11] P.B. Glaser, T.D. Tilley, J. Am. Chem. Soc. 125 (2003) 13640.
[12] L.W. Chung, Y.D. Wu, B.M. Trost, Z.T. Ball, J. Am. Chem. Soc. 125 (2003) 11578.
[13] B.M. Trost, Z.T. Ball, J. Am. Chem. Soc. 125 (2003) 30.
[14] B.M. Trost, Z.T. Ball, J. Am. Chem. Soc. 123 (2001) 12726.
[15] Y. Maruyama, K. Yamamura, T. Sagawa, H. Katayama, F. Ozawa, Organometallics 19 (2000) 1308.

[16] I. Ojima, T. Fuchikami, M. Yatabe, J. Organomet. Chem. 260 (1984) 335.
[17] Y. Maruyama, K. Yamamura, I. Nakayama, K. Yoshiuchi, F. Ozawa, J. Am. Chem. Soc. 120 (1998) 1421.
[18] B. Marciniec, C. Pietraszuk, Top. Organomet. Chem. 11 (2004) 197.
[19] T. Tuttle, D. Wang, W. Thiel, J. Köhler, M. Hofmann, J. Weis, Organometallics 25 (2006) 4504.
[20] A. Jansen, H. Gorls, S. Pitter, Organometallics 19 (2000) 135.
[21] A. Jansen, S. Pitter, J. Mol. Catal. A 217 (2004) 41.
[22] A.J. Chalk, J.F. Harrod, J. Am. Chem. Soc. 87 (1965) 16.
[23] M.J. Fernandez, M.A. Esteruelas, M.S. Jimenez, L.A. Oro, Organometallics 5 (1986) 1519.
[24] A. Onopchenko, E.T. Sabourin, D.L. Beach, J. Org. Chem. 48 (1983) 5101.
[25] C.L. Randolph, M.S. Wrighton, J. Am. Chem. Soc. 108 (1986) 3366.
[26] M.A. Schröder, M.S. Wrighton, J. Organomet. Chem. 128 (1977) 345.
[27] F. Seitz, M.S. Wrighton, Angew. Chem., Int. Ed. Engl. 27 (1988) 289.
[28] S. Sakaki, N. Mizoe, Y. Musashi, M. Sugimoto, J. Mol. Struct. (THEOCHEM) 462 (1999) 533.
[29] S. Sakaki, N. Mizoe, M. Sugimoto, Organometallics 17 (1998) 2510.
[30] S. Sakaki, N. Mizoe, M. Sugimoto, Y. Musashi, Coord. Chem. Rev. 192 (1999) 933.
[31] S. Sakaki, M. Ogawa, Y. Musashi, T. Arai, J. Am. Chem. Soc. 116 (1994) 7258.
[32] S. Sakaki, M. Sumimoto, M. Fukuhara, M. Sugimoto, H. Fujimoto, S. Matsuzaki, Organometallics 21 (2002) 3788.
[33] S.M. Maddock, C.E.F. Rickard, W.R. Roper, L.J. Wright, Organometallics 15 (1996) 1793.
[34] R.H. Crabtree, Chem. Rev. 95 (1995) 987.
[35] B.A. Arndtsen, R.G. Bergman, T.A. Mobley, T.H. Peterson, Acc. Chem. Res. 28 (1995) 154.
[36] P.F. Fu, L. Brard, Y.W. Li, T.J. Marks, J. Am. Chem. Soc. 117 (1995) 7157.
[37] M.R. Kesti, R.M. Waymouth, Organometallics 11 (1992) 1095.
[38] N.S. Radu, T.D. Tilley, J. Am. Chem. Soc. 117 (1995) 5863.
[39] A.Z. Voskoboynikov, I.N. Parshina, A.K. Shestakova, K.P. Butin, I.P. Beletskaya, L.G. Kuzmina, J.A.K. Howard, Organometallics 16 (1997) 4041.
[40] H.G. Woo, J.F. Walzer, T.D. Tilley, J. Am. Chem. Soc. 114 (1992) 7047.
[41] J.F. Hartwig, S. Bhandari, P.R. Rablen, J. Am. Chem. Soc. 116 (1994) 1839.
[42] F. Hutschka, A. Dedieu, M. Eichberger, R. Fornika, W. Leitner, J. Am. Chem. Soc. 119 (1997) 4432.
[43] C.N. Iverson, M.R. Smith, J. Am. Chem. Soc. 117 (1995) 4403.
[44] J.C. Lee, E. Peris, A.L. Rheingold, R.H. Crabtree, J. Am. Chem. Soc. 116 (1994) 11014.
[45] X.L. Luo, R.H. Crabtree, J. Am. Chem. Soc. 111 (1989) 2527.
[46] T.B. Marder, N.C. Norman, C.R. Rice, E.G. Robins, J. Chem. Soc., Chem. Commun. (1997) 53.
[47] F. Maseras, M. Duran, A. Lledos, J. Bertran, J. Am. Chem. Soc. 114 (1992) 2922.
[48] A. Milet, A. Dedieu, G. Kapteijn, G. van Koten, Inorg. Chem. 36 (1997) 3223.
[49] D.G. Musaev, A.M. Mebel, K. Morokuma, J. Am. Chem. Soc. 116 (1994) 10693.
[50] P.E.M. Siegbahn, R.H. Crabtree, J. Am. Chem. Soc. 118 (1996) 4442.
[51] M.D. Su, S.Y. Chu, J. Am. Chem. Soc. 119 (1997) 5373.
[52] V.G. Lakhtin, V.M. Nosova, A.V. Kisin, P.V. Ivanov, E.A. Chernyshev, Russ. J. Gen. Chem. 71 (2001) 1252.
[53] H. Watanabe, M. Asami, Y. Nagai, J. Organomet. Chem. 195 (1980) 363.
[54] B. Marciniec, H. Maciejewski, J. Gulinski, L. Rzejak, J. Organomet. Chem. 362 (1989) 273.
[55] W. Kohn, L.J. Sham, Phys. Rev. 140 (1965) 1133.
[56] R.G. Parr, W.T. Yang, Density Functional Theory of Atoms and Molecules, Oxford University Press, New York, 1989.
[57] D. Andrae, U. Häussermann, M. Dolg, H. Stoll, H. Preuss, Theor. Chim. Acta 77 (1990) 123.
[58] P.C. Hariharan, J.A. Pople, Theor. Chim. Acta 28 (1973) 213.
[59] W.J. Hehre, R. Ditchfield, J.A. Pople, J. Chem. Phys. 56 (1972) 2257.
[60] R. Ditchfield, W.J. Hehre, J.A. Pople, J. Chem. Phys. 54 (1971) 724.
[61] A.D. Becke, Phys. Rev. A 38 (1988) 3098.
[62] J.P. Perdew, Phys. Rev. B 33 (1986) 8822.
[63] S.H. Vosko, L. Wilk, M. Nusair, Can. J. Phys. 58 (1980) 1200.
[64] K. Eichkorn, O. Treutler, H. Ohm, M. Häser, R. Ahlrichs, Chem. Phys. Lett. 240 (1995) 283.
[65] TURBOMOLE, V. 5.7.1, COSMOlogic GmbH & Co. KG, Leverkusen, Germany, 2004.
[66] R. Ahlrichs, M. Bär, M. Häser, H. Horn, C. Kölmel, Chem. Phys. Lett. 162 (1989) 165.
[67] K. Eichkorn, O. Treutler, H. Ohm, M. Häser, R. Ahlrichs, Chem. Phys. Lett. 242 (1995) 652.
[68] O. Treutler, R. Ahlrichs, J. Chem. Phys. 102 (1995) 346.
[69] M.J. Frisch et al., GAUSSIAN-03, V.C.01, Gaussian, Inc., Wallingford, CT, 2004.
[70] A.D. Becke, J. Chem. Phys. 98 (1993) 5648.
[71] C.T. Lee, W.T. Yang, R.G. Parr, Phys. Rev. B 37 (1988) 785.
[72] P.J. Stephens, F.J. Devlin, C.F. Chabalowski, M.J. Frisch, J. Phys. Chem. 98 (1994) 11623.
[73] R.H. Hertwig, W. Koch, Chem. Phys. Lett. 268 (1997) 345.
[74] J. Baker, M. Muir, J. Andzelm, A. Scheiner, in: Chemical Applications Of Density Functional Theory, American Chemical Society Symposium, Washington, DC, 1996, p. 342.
[75] S.Q. Niu, M.B. Hall, Chem. Rev. 100 (2000) 353.
[76] S.E. Vyboishchikov, M. Bühl, W. Thiel, Chem. Eur. J. 8 (2002) 3962.
[77] C.Y. Peng, P.Y. Ayala, H.B. Schlegel, M.J. Frisch, J. Comput. Chem. 17 (1996) 49.
[78] C.Y. Peng, H.B. Schlegel, Isr. J. Chem. 33 (1993) 449.